

# Substantia Nigra Imaging in Parkinson

Subjects: **Medicine, General & Internal**

Contributor: Cesare Gagliardo , Paola Feraco , Jamir Pitton Rissardo

Parkinson's disease (PD) is a progressive neurodegenerative disorder, characterized by motor and non-motor symptoms due to the degeneration of the pars compacta of the substantia nigra (SNc) with dopaminergic denervation of the striatum. Although the diagnosis of PD is principally based on a clinical assessment, great efforts have been expended over the past two decades to evaluate reliable biomarkers for PD. Among these biomarkers, magnetic resonance imaging (MRI)-based biomarkers may play a key role. Conventional MRI sequences are considered by many in the field to have low sensitivity, while advanced pulse sequences and ultra-high-field MRI techniques have brought many advantages, particularly regarding the study of brainstem and subcortical structures. Nowadays, nigrosome imaging, neuromelanin-sensitive sequences, iron-sensitive sequences, and advanced diffusion weighted imaging techniques afford new insights to the non-invasive study of the SNc.

magnetic resonance imaging

neuromelanin

nigrosome-1

iron

biomarkers

radiomics

neurodegenerative diseases

Parkinson's disease

parkinsonian disorders

## 1. Introduction

Parkinson's disease (PD) is a progressive neurodegenerative disease that is characterized by motor and non-motor symptoms. The disease is mostly sporadic, and it is caused by the interplay between genetic and environmental factors [1]. The neuropathology of PD is characterized by neuronal degeneration in the pars compacta of the substantia nigra (SNc) with dopaminergic denervation of the striatum. Subsequently, this neuronal loss is also seen in other brain regions and non-dopaminergic neurons, with multisite involvement of the central, peripheral, and autonomic nervous system [2]. The histological hallmark of PD are Lewy bodies, which are cytoplasmic inclusions resulting from an abnormal deposition of  $\alpha$ -synuclein aggregates. The latter are not specific to PD, but they characterize other Parkinsonisms, such as Lewy body dementia and multiple system atrophy. It is currently unknown how Lewy bodies are related to the progression of PD, and current knowledge suggests that neuronal degeneration occurs due to several processes, including neuroinflammation, oxidative stress abnormalities, mitochondrial dysfunction, and abnormalities of protein quality control [3].

According to the *gut-to-brain* transmission model of PD pathology proposed by Braak et al., changes in brainstem and subcortical structures are more evident in early disease stages, while cortical structures are principally involved in advanced-stage PD [4]. Clinical manifestations of PD primarily include bradykinesia plus at least one of resting tremor and rigidity. Supportive criteria for a PD diagnosis are a beneficial response to dopamine therapy,

the presence of medication-induced dyskinesia, and (early) olfactory dysfunction [5]. Motor symptoms progressively worsen with age, leading to near total immobility in advanced-stage PD. Although PD has been primarily identified as a movement disorder, non-motor symptoms (such as hyposmia, autonomic dysfunction, mood and sleep disorders, and cognitive impairment) are very common features of the disease, and they have been associated with a poor quality of life [6]. Specifically, cognitive impairment—which encompasses a spectrum varying from mild cognitive impairment to dementia [7][8]—has been associated with poor outcomes and mortality [9].

The diagnosis of PD is to date based on clinical features, with motor symptoms constituting the core criteria [1][5]. Over the past two decades, great efforts have been invested in evaluating reliable biomarkers for PD; none of these parameters, however, have been successfully validated for routine clinical practice [10]. Among these biomarkers, magnetic resonance imaging (MRI)-based biomarkers have undoubtedly contributed to the differential diagnosis between degenerative from secondary Parkinsonism [11].

## 2. Neuromelanin Imaging

Neuromelanin (NM) is a black pigment that is composed of melanin, proteins, lipids, and metal ions, and it is found in the SNc (in the nigral matrix and the nigrosomes). NM plays a protective role against the accumulation of toxic catecholamine derivatives and oxidative stress [12]. NM normally accumulates during aging but is strongly reduced in patients with PD as a result of the selective loss of dopaminergic neurons containing NM. The latter has a paramagnetic T1 reduction effect on MRI due to the presence of melanin-iron complexes [13]. With high-resolution turbo spin echo (TSE) T1W images with a magnetization transfer (MT) pulse, it is possible to suppress brain tissue signals due to the prolongation of the T1 relaxation time [14]. Hence, nuclei-containing NM can be visualized as a separate hyperintense area relative to the surrounding hypointense brain tissue. Although the use of TSE T1W images has been consistently applied to visualizing NM, the gradient recalled echo (GRE) sequence with MT pulse has recently been demonstrated to achieve the sharpest contrast and lowest variability when compared with a T1W TSE-MT sequence [15].

NM-MRI is a validated technique with which to quantify the loss of dopaminergic neurons in the SN of patients with PD. The loss of SN hyperintensity in the T1W-MT sequence is associated with the loss of neuromelanin-containing neurons in PD and DLB, as confirmed in post-mortem studies [16]. Indeed, patients suffering from PD have significantly reduced NM signal in the SN (**Figure 2**), which invariably decreases on follow-up [17][18][19][20][21][22].



**Figure 2.** NM-MRI sequence with an explicit MT preparation pulse, scanned with a 1.5T MR scanner at the level of the SN in a PD patient with asymmetrical motor symptoms onset: the loss of hyperintensity in the posterolateral aspect of the right SN (arrow) correlated well with the clinical presentation.

Measuring NM-sensitive images correlates with elevated diagnostic accuracy for PD: the sensitivity and specificity of this technique to distinguish between PD and control patients are 88% and 80%, respectively [23]. The NM signal changes commence in the posterolateral motor areas of the SN, and then proceed to the medial areas [24]. Hence, the evaluation of longitudinal changes in the NM signal in PD patients could be used as a marker indicating disease progression. A reduction in NM signal has been reported to be not specific for motor or non-motor PD subtypes [25]. On the other hand, a potential diagnostic value of NM-MRI in discriminating PD motor phenotypes has been proposed [26]. Indeed, patients with postural instability gait difficulty phenotype display increased severe signal attenuation in the medial part of the SNC, in comparison with tremor-dominant PD patients [26]. Furthermore, the use of NM-MRI-based imaging is capable of differentiating between untreated essential tremor (ET) and de novo PD with a tremor-dominant phenotype [27]. Finally, a NM signal decrease has been observed in patients suffering from idiopathic rapid eye movement sleep behavior disorder, which is considered a prodromal phase of Parkinsonism and PD [28][29].

### 3. Nigrosome-1 Imaging

Nigrosomes are dopaminergic neurons within the SNC that are characterized by high NM levels and a paucity of iron. They can be subdivided into five different regions (nigrosome 1 to 5), the largest of which, nigrosome-1 (located in the dorsolateral part of SNC [30]), has been shown to play a key role in the neuropathology of PD. Indeed, the greatest loss of dopaminergic neurons in PD patients occurs in the nigrosome-1. It was first detected in vivo by 7.0-Tesla (7T) MRI as a hyperintense, ovoid area on T2\*-weighted images, within the dorsolateral border of the hypointense SN pars compacta [31][32]. Similar findings can be found with the more commonly used 3-Tesla (3T) MRI [33]. By using T2\* or susceptibility-weighted imaging (SWI), researchers have also termed this region *dorsolateral nigral hyperintensity* or a *swallow-tail sign* (STS) (Figure 3).

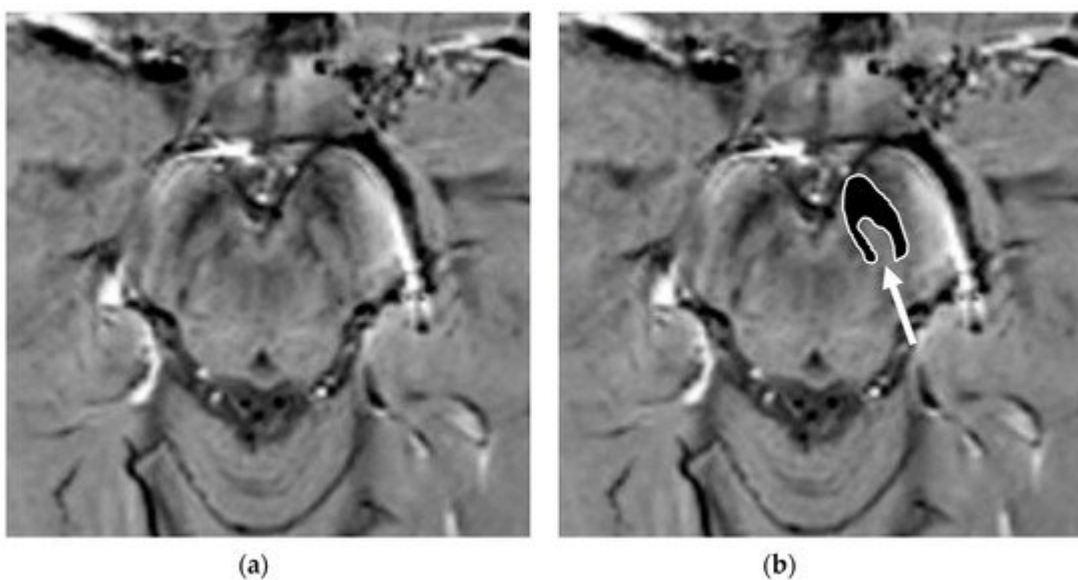


**Figure 3.** Susceptibility-weighted imaging (SWI) scan performed with a 3T MR scanner in a normally aging brain of a 65-year-old male who underwent a brain MRI examination for persistent headaches. A raw slice passing through the mesencephalon (a) and the same slice with superimposed highlighted SNC (white surrounded black ROI), thereby demonstrating the normal appearance of the nigrosome-1 (hyperintense area pointed by the white arrow) or swallow-tail sign (b).

Normal nigrosome-1 and the surrounding structure of the dorsolateral SN appear as a swallow tail [34], and they can be visualized in 95% of healthy subjects [35][36]. Iron deposits and microvessels have been reported as contributing to the hyposignal surrounding nigrosome-1 in the SWI of normal aged midbrains [37]. Nigrosome-1 in PD patients displays a significant loss of STS on T2\* weighted images, probably due to a reduction in NM within dopaminergic neurons, an increase in free iron (which induces local inhomogeneity in the magnetic field resulting in signal loss), or a loss of paramagnetic NM–iron complexes [38][39]. As the disease advances, a loss of T2\* hyperintensity in PD has been demonstrated to progress from nigrosome-1 to nigrosome-4 [40]. The absence of STS may assist in the differential diagnosis for PD if compared with controls and ET, ultimately reaching high sensitivity and specificity [41][34][42][43] (Figure 4).

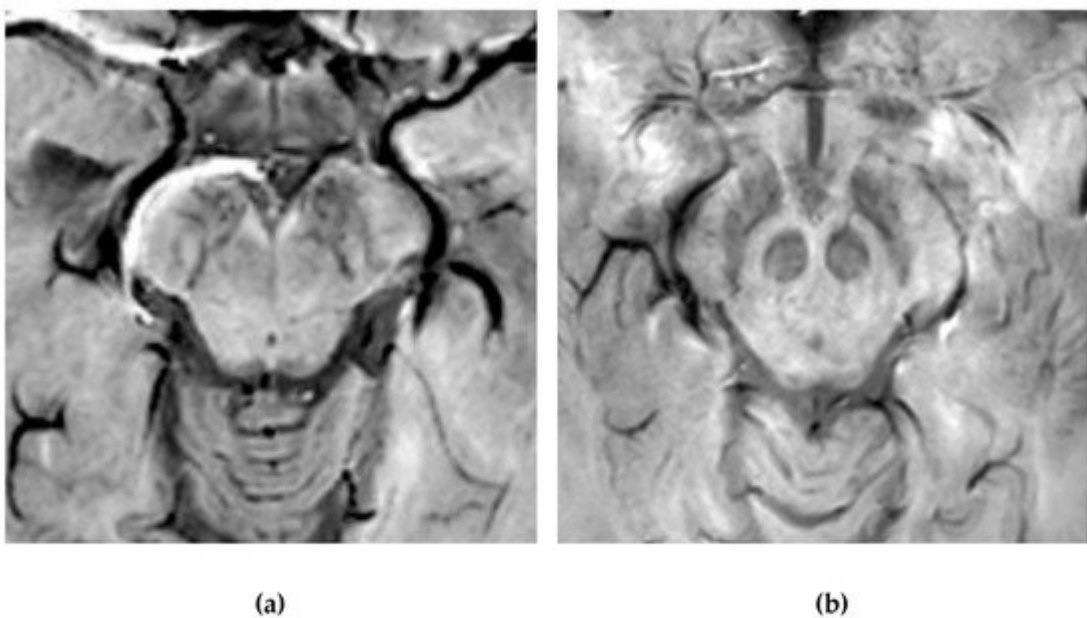


**Figure 4.** Susceptibility-weighted imaging (SWI) scan performed with a 3T MR. (a) Presence of regular swallow tail sign in a healthy patient; (b) loss of swallow tail sign in a patient with Parkinson's disease.

Moreover, the imaging of nigrosome-1 with 3T MR has been demonstrated to differentiate drug-induced Parkinsonism from idiopathic PD with elevated accuracy, thereby being of assistance in screening patients who required dopamine transporter imaging [44]. Furthermore, a loss of STS has also been observed in patients suffering from idiopathic rapid eye movement sleep behavior disorder and DLB [45][46]. Whilst the loss of nigrosome-1 on SWI sequences may assist as a potential imaging biomarker in the diagnosis of degenerative parkinsonian syndromes, it cannot differentiate between idiopathic PD and PS [47][48]. Nevertheless, it has been reported that anatomical changes of SN, detected via the SWI sequence at 7T, may distinguish MSA and PSP from CBD [49], thereby confirming the pathological heterogeneity of these diseases. Of note, nigrosome-1 has also been visualized on 3D FLAIR images as an hyperintense structure within otherwise surrounding hypointense dorsolateral SN. Its loss can be used to predict presynaptic dopaminergic function and to diagnose PD with a high degree of accuracy [50].

Recently, it has been reported that the combined visual analysis of SN (by using NM-MRI and nigrosome-1 imaging, displaying normal NM in SNC and nigrosome-1 loss) has enabled the distinction of MSA-P from PD and healthy controls [51]. Moreover, it has also been described that a stratification of the swallow tail sign, using a scale on SWI-map imaging, may serve as a useful imaging biomarker regarding the differential diagnosis of Parkinsonism [52]. However, the veracity of these results must be confirmed by larger cohort studies.

It is important to note that adequate visualization of the swallow tail sign requires targeted 3D high-resolution SWI. In the original publication, the parameters were: FEEPI, TR/TE 60/30, echo train length 5, flip angle 19°; 70 slices; voxel size 0.55 x 0.55 x 0.7 mm. [53]

## 4. Iron Imaging

Together with a degeneration of dopaminergic neurons, iron overload has been implicated in the pathology and pathogenesis of PD and PS. Iron deposition initially occurs in SN; however, abnormal iron levels have also been detected in the basal ganglia, thalamus, and cortex of PD patients [54].

With the introduction of MRI, the *in vivo* characterization of brain iron content has become possible. The possibility of quantifying regional brain iron overload may provide more knowledge regarding the correlation between iron accumulation and parkinsonian symptoms. Indeed, extensive data have emphasized the importance of SN iron increase in PD patients compared to controls [23][28][55]. From a technical perspective, the iron content can be assessed by evaluating T2 and T2\* relaxation rates, using either magnitude (R2\*) or phase (quantitative susceptibility mapping, QSM) imaging. Among these methods, R2 and R2\* relaxometry (i.e.,:  $1/T2^*$ , proton transverse relaxation rate which reflects increased tissue iron content) considers heterogeneities from local and adjacent tissue as being more susceptible to influence from disturbances due to calcification, micro bleeds, and myelinated fibers [11]. The R2\* values in the SNC have been reported to be significantly higher in de novo PD patients with a gradual increase, which is related to disease progression [56][57] (Figure 5).

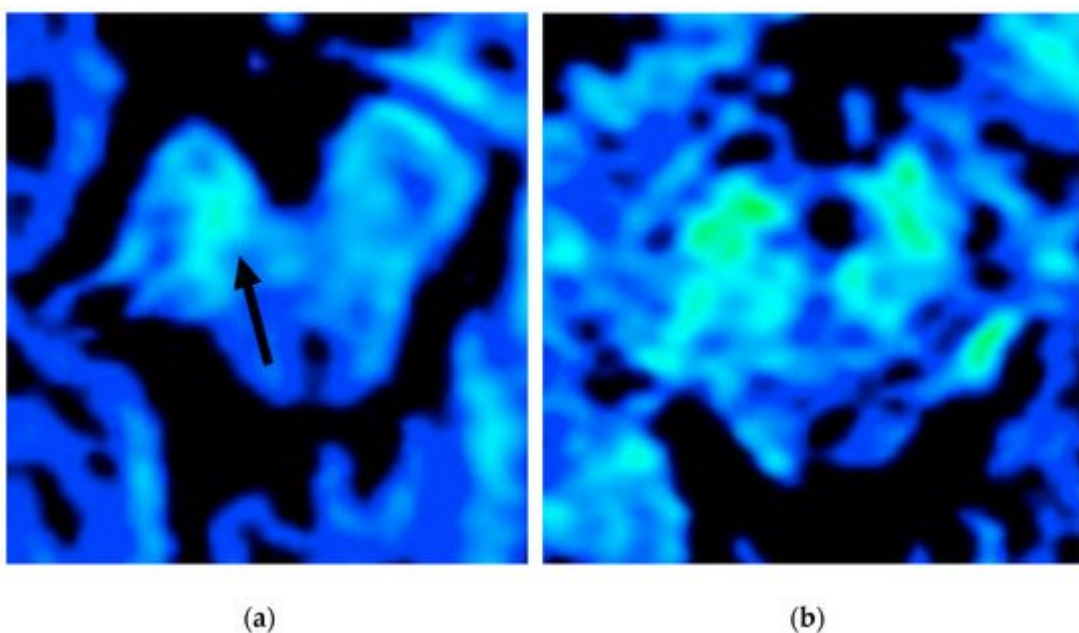


**Figure 5.** T2\* map study (color scale) of two patients with PD in an evaluation of iron deposition within the SN (blue: less iron deposition; green: more iron deposition). The patient in (a) has a more evident asymmetrical iron deposition when compared to the patient in (b).

Since correlations between motor symptoms and high levels of R2\* values within the SNC have been reported in PD, and R2\* changes rapidly with disease progression, these methods can also be used in the prospective evaluation of PD patients [56][57]. Moreover, it has been reported that PD patients with early gait freezing pattern will have higher iron content, as evaluated by means of R2\* relaxometry in the SNC, in comparison to those who do not [58].

Furthermore, QSM provides a direct measure of the local heterogeneities of the magnetic field by using a deconvolution method, which assists in eliminating the susceptibilities of surrounding structures [59]. It has been demonstrated that QSM is more sensitive than R2\* in identifying iron overload in PD [59][60][61], even in the prodromal stage of the disease [62]. Values from QSM correlate with disease condition and duration [60][61][63][64], and they distinguish PD and PS [65]. Moreover, QSM can address iron variation within the SN [66] and lateral asymmetry of iron deposition, which is related to a manifestation of asymmetric signs and symptoms in PD [17]. When QSM is used in early- and advanced-stage PD patients, it is of note that it has been demonstrated that iron deposition affected SNc exclusively in the early stages of the disease, while in the late PD stage, iron deposition involved other regions, concomitant with SNc [67]. This latter finding indicates that QSM is a tool with which to monitor iron deposition and disease progression in PD. Specifically, changes in iron seem to be limited to the ventral aspect of SN [66], which has been reported to degenerate early in the course of the disease [68]. According to the distribution of the pathological involvement distinguishing the various forms of Parkinsonism, red and subtalamic nuclei are involved in PSP, together with SN, while iron deposition in MSA is significantly higher in the putamen [69]. Finally, all Parkinsonisms have been demonstrated to display increased susceptibility in the subcortical structures, thereby reflecting distinct topographical patterns of abnormal brain iron accumulation [70].

Both QSM and R2\* may be effective tools in the differential diagnoses of degenerative PS, a fact that permits the tracking of dynamic changes that are associated with the pathological progression of these disorders. In addition, while QSM is more sensitive to the iron content of SN, R2\* can be said to reflect pathological features, such as  $\alpha$ -synuclein, in addition to iron deposits [71].

## References

1. Kalia, L.V.; Lang, A.E. Parkinson's disease. *Lancet* 2015, 386, 896–912.
2. Dickson, D.W. Neuropathology of Parkinson disease. *Park. Relat. Disord.* 2018, 46, S30–S33.
3. Cacabelos, R. Parkinson's Disease: From Pathogenesis to Pharmacogenomics. *Int. J. Mol. Sci.* 2017, 18, 551.
4. Braak, H.; Ghebremedhin, E.; Rüb, U.; Bratzke, H.; Del Tredici, K. Stages in the development of Parkinson's disease-related pathology. *Cell Tissue Res.* 2004, 318, 121–134.
5. Postuma, R.B.; Berg, D.; Stern, M.B.; Poewe, W.; Olanow, C.W.; Oertel, W.H.; Obeso, J.; Marek, K.; Litvan, I.; Lang, A.E.; et al. MDS clinical diagnostic criteria for Parkinson's disease. *Mov. Disord.* 2015, 30, 1591–1601.
6. Schapira, A.H.; Chaudhuri, K.R.; Jenner, P. Non-motor features of Parkinson disease. *Nat. Rev. Neurosci.* 2017, 18, 435–450.
7. Monastero, R.; Cicero, C.E.; Baschi, R.; Davì, M.; Luca, A.; Restivo, V.; Zangara, C.; Fierro, B.; Zappia, M.; Nicoletti, A. Mild cognitive impairment in Parkinson's disease: The Parkinson's

disease cognitive study (PACOS). *J. Neurol.* 2018, **265**, 1050–1058.

8. Nicoletti, A.; Luca, A.; Baschi, R.; Cicero, C.E.; Mostile, G.; Davì, M.; Pilati, L.; Restivo, V.; Zappia, M.; Monastero, R. Incidence of Mild Cognitive Impairment and Dementia in Parkinson’s Disease: The Parkinson’s Disease Cognitive Impairment Study. *Front. Aging Neurosci.* 2019, **11**, 21.

9. Aarsland, D.; Creese, B.; Politis, M.; Chaudhuri, K.R.; Ffytche, D.H.; Weintraub, D.; Ballard, C. Cognitive decline in Parkinson disease. *Nat. Rev. Neurol.* 2017, **13**, 217–231.

10. Chen-Plotkin, A.S.; Albin, R.; Alcalay, R.; Babcock, D.; Bajaj, V.; Bowman, D.; Buko, A.; Cedarbaum, J.; Chelsky, D.; Cookson, M.R.; et al. Finding useful biomarkers for Parkinson’s disease. *Sci. Transl. Med.* 2018, **10**, eaam6003.

11. Heim, B.; Krismer, F.; De Marzi, R.; Seppi, K. Magnetic resonance imaging for the diagnosis of Parkinson’s disease. *J. Neural Transm.* 2017, **124**, 915–964.

12. Zucca, F.A.; Basso, E.; Cupaioli, F.A.; Ferrari, E.; Sulzer, D.; Casella, L.; Zecca, L. Neuromelanin of the Human Substantia Nigra: An Update. *Neurotox. Res.* 2014, **25**, 13–23.

13. Trujillo, P.; Summers, P.; Ferrari, E.; Zucca, F.A.; Sturini, M.; Mainardi, L.T.; Cerutti, S.; Smith, A.K.; Smith, S.A.; Zecca, L.; et al. Contrast mechanisms associated with neuromelanin-MRI. *Magn. Reson. Med.* 2017, **78**, 1790–1800.

14. Sasaki, M.; Shibata, E.; Kudo, K.; Tohyama, K. Neuromelanin-sensitive MRI basics, technique, and clinical applications. *Clin. Neuroradiol.* 2008, **18**, 147–153.

15. Pluijm, M.; Cassidy, C.; Ms, M.Z.; Wallert, E.; Bruin, K.; Booij, J.; Haan, L.; Horga, G.; Giessen, E. Reliability and Reproducibility of Neuromelanin-Sensitive Imaging of the Substantia Nigra: A Comparison of Three Different Sequences. *J. Magn. Reson. Imaging* 2021, **53**, 712–721.

16. Kitao, S.; Matsusue, E.; Fujii, S.; Miyoshi, F.; Kaminou, T.; Kato, S.; Ito, H.; Ogawa, T. Correlation between pathology and neuromelanin MR imaging in Parkinson’s disease and dementia with Lewy bodies. *Neuroradiology* 2013, **55**, 947–953.

17. Reimão, S.; Lobo, P.P.; Neutel, D.; Guedes, L.C.; Coelho, M.; Rosa, M.M.; Azevedo, P.; Ferreira, J.; Abreu, D.; Gonçalves, N.; et al. Substantia nigra neuromelanin-MR imaging differentiates essential tremor from Parkinson’s disease. *Mov. Disord.* 2015, **30**, 953–959.

18. Sulzer, D.; Cassidy, C.; Horga, G.; Kang, U.J.; Fahn, S.; Casella, L.; Pezzoli, G.; Langley, J.; Hu, X.P.; Zucca, F.A.; et al. Neuromelanin detection by magnetic resonance imaging (MRI) and its promise as a biomarker for Parkinson’s disease. *NPJ Park. Dis.* 2018, **4**, 1–13.

19. Matsuura, K.; Maeda, M.; Tabei, K.-I.; Umino, M.; Kajikawa, H.; Satoh, M.; Kida, H.; Tomimoto, H. A longitudinal study of neuromelanin-sensitive magnetic resonance imaging in Parkinson’s disease. *Neurosci. Lett.* 2016, **633**, 112–117.

20. Takahashi, H.; Watanabe, Y.; Tanaka, H.; Mihara, M.; Mochizuki, H.; Yamamoto, K.; Liu, T.; Wang, Y.; Tomiyama, N. Comprehensive MRI quantification of the substantia nigra pars compacta in Parkinson's disease. *Eur. J. Radiol.* 2018, 109, 48–56.

21. Takahashi, H.; Watanabe, Y.; Tanaka, H.; Mihara, M.; Mochizuki, H.; Liu, T.; Wang, Y.; Tomiyama, N. Quantifying changes in nigrosomes using quantitative susceptibility mapping and neuromelanin imaging for the diagnosis of early-stage Parkinson's disease. *Br. J. Radiol.* 2018, 91, 20180037.

22. Prasad, S.; Stezin, A.; Lenka, A.; George, L.; Saini, J.; Yadav, R.; Pal, P.K. Three-dimensional neuromelanin-sensitive magnetic resonance imaging of the substantia nigra in Parkinson's disease. *Eur. J. Neurol.* 2018, 25, 680–686.

23. Pyatigorskaya, N.; Magnin, B.; Mongin, M.; Yahia-Cherif, L.; Valabregue, R.; Arnaldi, D.; Ewenczyk, C.; Poupon, C.; Vidailhet, M.; Lehéricy, S. Comparative Study of MRI Biomarkers in the Substantia Nigra to Discriminate Idiopathic Parkinson Disease. *Am. J. Neuroradiol.* 2018, 39, 1460–1467.

24. Biondetti, E.; Gaurav, R.; Yahia-Cherif, L.; Mangone, G.; Pyatigorskaya, N.; Valabregue, R.; Ewenczyk, C.; Hutchison, M.; François, C.; Arnulf, I.; et al. Spatiotemporal changes in substantia nigra neuromelanin content in Parkinson's disease. *Brain* 2020, 143, 2757–2770.

25. Wang, J.; Li, Y.; Huang, Z.; Wan, W.; Zhang, Y.; Wang, C.; Cheng, X.; Ye, F.; Liu, K.; Fei, G.; et al. Neuromelanin-sensitive magnetic resonance imaging features of the substantia nigra and locus caeruleus in de novo Parkinson's disease and its phenotypes. *Eur. J. Neurol.* 2018, 25, 949–e73.

26. Xiang, Y.; Gong, T.; Wu, J.; Li, J.; Chen, Y.; Wang, Y.; Li, S.; Cong, L.; Lin, Y.; Han, Y.; et al. Subtypes evaluation of motor dysfunction in Parkinson's disease using neuromelanin-sensitive magnetic resonance imaging. *Neurosci. Lett.* 2017, 638, 145–150.

27. Wang, J.; Huang, Z.; Li, Y.; Ye, F.; Wang, C.; Zhang, Y.; Cheng, X.; Fei, G.; Liu, K.; Zeng, M.; et al. Neuromelanin-sensitive MRI of the substantia nigra: An imaging biomarker to differentiate essential tremor from tremor-dominant Parkinson's disease. *Parkinsonism Relat. Disord.* 2019, 58, 3–8.

28. Chougar, L.; Pyatigorskaya, N.; Degos, B.; Grabli, D.; Lehéricy, S. The Role of Magnetic Resonance Imaging for the Diagnosis of Atypical Parkinsonism. *Front. Neurol.* 2020, 11, 665.

29. Pyatigorskaya, N.; Gaurav, R.; Arnaldi, D.; Leu-Semenescu, S.; Yahia-Cherif, L.; Valabregue, R.; Vidailhet, M.; Arnulf, I.; Lehéricy, S. Magnetic Resonance Imaging Biomarkers to Assess Substantia Nigra Damage in Idiopathic Rapid Eye Movement Sleep Behavior Disorder. *Sleep* 2017, 40.

30. Damier, P.; Hirsch, E.C.; Agid, Y.; Graybiel, A.M. The substantia nigra of the human brain. I. Nigrosomes and the nigral matrix, a compartmental organization based on calbindin D(28K) immunohistochemistry. *Brain* 1999, 122, 1421–1436.

31. Schwarz, S.T.; Mougin, O.; Xing, Y.; Blazejewska, A.; Bajaj, N.; Auer, D.P.; Gowland, P. Parkinson's disease related signal change in the nigrosomes 1–5 and the substantia nigra using T2\* weighted 7T MRI. *NeuroImage Clin.* 2018, **19**, 683–689.

32. Lehéricy, S.; Bardinet, E.; Poupon, C.; Vidailhet, M.; François, C. 7 tesla magnetic resonance imaging: A closer look at sub-stantia nigra anatomy in Parkinson's disease. *Mov Disord* 2014, **29**, 1574–1581.

33. Schwarz, S.T.; Afzal, M.; Morgan, P.S.; Bajaj, N.; Gowland, P.A.; Auer, D.P. The “swallow tail” appearance of the healthy nigro-some—A new accurate test of Parkinson's disease: A case-control and retrospective cross-sectional MRI study at 3T. *PLoS ONE* 2014, **9**, 93814.

34. Gao, P.; Zhou, P.-Y.; Wang, P.-Q.; Zhang, G.-B.; Liu, J.-Z.; Xu, F.; Yang, F.; Wu, X.-X.; Li, G. Universality analysis of the existence of substantia nigra “swallow tail” appearance of non-Parkinson patients in 3T SWI. *Eur. Rev. Med. Pharmacol. Sci.* 2016, **20**, 1307–1314.

35. Cheng, Z.; He, N.; Huang, P.; Li, Y.; Tang, R.; Sethi, S.K.; Ghassaban, K.; Yerramsetty, K.K.; Palutla, V.K.; Chen, S.; et al. Imaging the Nigrosome 1 in the substantia nigra using sus-ceptibility weighted imaging and quantitative susceptibility mapping: An application to Parkinson's disease. *NeuroImage Clin.* 2020, **25**, 102–103.

36. Schmidt, M.A.; Engelhorn, T.; Marxreiter, F.; Winkler, J.; Lang, S.; Kloska, S.; Goelitz, P.; Doerfler, A. Ultra high-field SWI of the substantia nigra at 7T: Reliability and consistency of the swallow-tail sign. *BMC Neurol.* 2017, **17**, 1–6.

37. Kau, T.; Hametner, S.; Endmayr, V.; Deistung, A.; Prihoda, M.; Haimburger, E.; Menard, C.; Haider, T.; Höftberger, R.; Robinson, S.; et al. Microvessels may Confound the “Swallow Tail Sign” in Normal Aged Midbrains: A Postmortem 7 T SW-MRI Study. *J. Neuroimaging* 2018, **29**, 65–69.

38. Gao, P.; Zhou, P.-Y.; Li, G.; Zhang, G.-B.; Wang, P.-Q.; Liu, J.-Z.; Xu, F.; Yang, F.; Wu, X.-X. Visualization of nigrosomes-1 in 3T MR susceptibility weighted imaging and its absence in diagnosing Parkinson's disease. *Eur. Rev. Med. Pharmacol. Sci.* 2015, **19**, 4603–4609.

39. Mahlknecht, P.; Krismer, F.; Poewe, W.; Seppi, K. Meta-analysis of dorsolateral nigral hyperintensity on magnetic reso-nance imaging as a marker for Parkinson's disease. *Mov. Disord.* 2017, **32**, 619–623.

40. Sung, Y.H.; Lee, J.; Nam, Y.; Shin, H.-G.; Noh, Y.; Shin, D.H.; Kim, E.Y. Differential involvement of nigral subregions in idiopathic parkinson's disease. *Hum. Brain Mapp.* 2018, **39**, 542–553.

41. Akly, M.S.P.; Stefani, C.V.; Ciancaglini, L.; Bestoso, J.S.; Funes, J.A.; Bauso, D.J.; Besada, C.H. Accuracy of nigrosome-1 detection to discriminate patients with Parkinson's disease and essential tremor. *Neuroradiol. J.* 2019, **32**, 395–400.

42. Calloni, S.F.; Conte, G.; Sbaraini, S.; Cilia, R.; Contarino, V.E.; Avignone, S.; Sacilotto, G.; Pezzoli, G.; Triulzi, F.M.; Scola, E. Multiparametric MR imaging of Parkin-sonisms at 3 tesla: Its

role in the differentiation of idiopathic Parkinson's disease versus atypical Parkinsonian disorders. *Eur. J. Radiol.* 2018, 109, 95–100.

43. Stezin, A.; Naduthota, R.M.; Botta, R.; Varadharajan, S.; Lenka, A.; Saini, J.; Yadav, R.; Pal, P.K. Clinical utility of visualisation of nigro-some-1 in patients with Parkinson's disease. *Eur. Radiol.* 2018, 28, 718–726.

44. Sung, Y.H.; Noh, Y.; Lee, J.; Kim, E.Y. Drug-induced Parkinsonism versus Idiopathic Parkinson Disease: Utility of Nigro-some 1 with 3-T Imaging. *Radiology* 2016, 279, 849–858.

45. De Marzi, R.; Seppi, K.; Högl, B.; Müller, C.; Scherfler, C.; Stefani, A.; Iranzo, A.; Tolosa, E.; Santamaría, J.; Gizewski, E.R.; et al. Loss of dorsolateral nigral hyperintensity on 3.0 tesla susceptibility-weighted imaging in idiopathic rapid eye movement sleep behavior disorder. *Ann. Neurol.* 2016, 79, 1026–1030.

46. Rizzo, G.; De Blasi, R.; Capozzo, R.; Tortelli, R.; Barulli, M.R.; Liguori, R.; Grasso, D.; Logroscino, G. Loss of Swallow Tail Sign on Susceptibility-Weighted Imaging in Dementia with Lewy Bodies. *J. Alzheimers Dis.* 2019, 67, 61–65.

47. Kathuria, H.; Mehta, S.; Ahuja, C.K.; Chakravarty, K.; Ray, S.; Mittal, B.R.; Singh, P.; Lal, V. Utility of Imaging of Nigrosome-1 on 3T MRI and Its Comparison with 18F-DOPA PET in the Diagnosis of Idiopathic Parkinson Disease and Atypical Parkinsonism. *Mov. Disord. Clin. Pr.* 2021, 8, 224–230.

48. Kim, J.-M.; Jeong, H.-J.; Bae, Y.J.; Park, S.-Y.; Kim, E.; Kang, S.Y.; Oh, E.S.; Kim, K.J.; Jeon, B.; Kim, S.E.; et al. Loss of substantia nigra hyperintensity on 7 Tesla MRI of Parkinson's disease, multiple system atrophy, and progressive supranuclear palsy. *Park. Relat. Disord.* 2016, 26, 47–54.

49. Frosini, D.; Ceravolo, R.; Tosetti, M.; Bonuccelli, U.; Cosottini, M. Nigral involvement in atypical parkinsonisms: Evidence from a pilot study with ultra-high field MRI. *J. Neural Transm.* 2016, 123, 509–513.

50. Oh, S.W.; Shin, N.Y.; Lee, J.J.; Lee, S.K.; Lee, P.H.; Lim, S.M.; Kim, J.W. Correlation of 3D FLAIR and Dopamine Transporter Imaging in Patients With Parkinsonism. *AJR Am. J. Roentgenol.* 2016, 207, 1089–1094.

51. Simões, R.M.; Caldas, A.C.; Grilo, J.; Correia, D.; Guerreiro, C.; Lobo, P.P.; Valadas, A.; Fabbri, M.; Guedes, L.C.; Coelho, M.; et al. A distinct neuromelanin magnetic resonance imaging pattern in parkinsonian multiple system atrophy. *BMC Neurol.* 2020, 20, 1–12.

52. Vitali, P.; Pan, M.I.; Palesi, F.; Germani, G.; Faggioli, A.; Anzalone, N.; Francaviglia, P.; Minafra, B.; Zangaglia, R.; Pacchetti, C.; et al. Substantia Nigra Volumetry with 3-T MRI in De Novo and Advanced Parkinson Disease. *Radiology* 2020, 296, 401–410.

53. Malte Brammerloh; Evgeniya Kirilina; Anneke Alkemade; Pierre-Louis Bazin; Caroline Jantzen; Carsten Jäger; Andreas Herrler; Kerrin J. Pine; Penny A. Gowland; Markus Morawski; et al. Birte U. Forstmann Nikolaus Weiskopf Swallow Tail Sign: Revisited. *Radiol.* **2022**, *305*, 674–677.

54. Wang, J.Y.; Zhuang, Q.Q.; Zhu, L.B.; Zhu, H.; Li, T.; Li, R.; Chen, S.F.; Huang, C.P.; Zhang, X.; Zhu, J.H. Meta-analysis of brain iron levels of Parkinson's disease patients determined by postmortem and MRI measurements. *Sci. Rep.* **2016**, *6*, 36669.

55. Wang, Y.; Butros, S.R.; Shuai, X.; Dai, Y.; Chen, C.; Liu, M.; Haacke, E.M.; Hu, J.; Xu, H. Different iron-deposition patterns of multiple system atrophy with predominant parkinsonism and idiopathic Parkinson diseases demonstrated by phase-corrected susceptibility-weighted imaging. *AJNR Am. J. Neuroradiol.* **2012**, *33*, 266–273.

56. Hopes, L.; Grolez, G.; Moreau, C.; Lopes, R.; Ryckewaert, G.; Carrière, N.; Auger, F.; Laloux, C.; Petrault, M.; Devedjian, J.-C.; et al. Magnetic Resonance Imaging Features of the Nigrostriatal System: Biomarkers of Parkinson's Disease Stages? *PLoS ONE* **2016**, *11*, e0147947.

57. Du, G.; Lewis, M.M.; Sica, C.; He, L.; Connor, J.R.; Kong, L.; Mailman, R.B.; Huang, X. Distinct progression pattern of susceptibility MRI in the substantia nigra of Parkinson's patients. *Mov. Disord.* **2018**, *33*, 1423–1431.

58. Wieler, M.; Gee, M.; Camicioli, R.; Martin, W.W. Freezing of gait in early Parkinson's disease: Nigral iron content estimated from magnetic resonance imaging. *J. Neurol. Sci.* **2016**, *361*, 87–91.

59. Du, G.; Liu, T.; Lewis, M.M.; Kong, L.; Wang, Y.; Connor, J.; Mailman, R.B.; Huang, X. Quantitative susceptibility mapping of the midbrain in Parkinson's disease. *Mov. Disord.* **2016**, *31*, 317–324.

60. Azuma, M.; Hirai, T.; Yamada, K.; Yamashita, S.; Ando, Y.; Tateishi, M.; Iryo, Y.; Yoneda, T.; Kitajima, M.; Wang, Y.; et al. Lateral asymmetry and spatial difference of iron deposition in the substantia nigra of patients with Parkinson disease measured with quantitative susceptibility mapping. *AJNR Am. J. Neuroradiol.* **2016**, *37*, 782–788.

61. Langkammer, C.; Pirpamer, L.; Seiler, S.; Deistung, A.; Schweser, F.; Franthal, S.; Homayoon, N.; Katschnig-Winter, P.; Koegl-Wallner, M.; Pendl, T.; et al. Quantitative Susceptibility Mapping in Parkinson's Disease. *PLoS ONE* **2016**, *11*, e0162460.

62. Sun, J.; Lai, Z.; Ma, J.; Gao, L.; Chen, M.; Chen, J.; Fang, J.; Fan, Y.; Bao, Y.; Zhang, D.; et al. Quantitative Evaluation of Iron Content in Idiopathic Rapid Eye Movement Sleep Behavior Disorder. *Mov. Disord.* **2020**, *35*, 478–485.

63. Saikiran, P.; Priyanka. Effectiveness of QSM over R2\* in assessment of parkinson's disease—A systematic review. *Neurol. India.* **2020**, *68*, 278–281.

64. An, H.; Zeng, X.; Niu, T.; Li, G.; Yang, J.; Zheng, L.; Zhou, W.; Liu, H.; Zhang, M.; Huang, D.; et al. Quantifying iron deposition within the substantia nigra of Parkinson's disease by quantitative

susceptibility mapping. *J. Neurol. Sci.* 2018, 386, 46–52.

65. Fedeli, M.P.; Contarino, V.E.; Siggillino, S.; Samoylova, N.; Calloni, S.; Melazzini, L.; Conte, G.; Sacilotto, G.; Pezzoli, G.; Triulzi, F.M.; et al. Iron deposition in Parkinsonisms: A Quantitative Susceptibility Mapping study in the deep grey matter. *Eur. J. Radiol.* 2020, 133, 109394.

66. Bergsland, N.; Zivadinov, R.; Schweser, F.; Hagemeier, J.; Licher, D.; Guttuso, T., Jr. Ventral posterior substantia nigra iron increases over 3 years in Parkinson's disease. *Mov. Disord.* 2019, 34, 1006–1013.

67. Guan, X.; Xuan, M.; Gu, Q.; Huang, P.; Liu, C.; Wang, N.; Xu, X.; Luo, W.; Zhang, M. Regionally progressive accumulation of iron in Parkinson's disease as measured by quantitative susceptibility mapping. *NMR Biomed.* 2017, 30, e3489.

68. Damier, P.; Hirsch, E.C.; Agid, Y.; Graybiel, A.M. The substantia nigra of the human brain. II. Patterns of loss of dopa-mine-containing neurons in Parkinson's disease. *Brain* 1999, 122, 1437–1448.

69. Mazzucchi, S.; Frosini, D.; Costagli, M.; Del Prete, E.; Donatelli, G.; Cecchi, P.; Migaleddu, G.; Bonuccelli, U.; Ceravolo, R.; Cosottini, M. Quantitative susceptibility mapping in atypical Parkinsonisms. *NeuroImage Clin.* 2019, 24, 101999.

70. Sjöström, H.; Granberg, T.; Westman, E.; Svenningsson, P. Quantitative susceptibility mapping differentiates between parkinsonian disorders. *Parkinsonism Relat. Disord.* 2017, 44, 51–57.

71. Lewis, M.M.; Du, G.; Baccon, J.; Snyder, A.M.; Murie, B.; Cooper, F.; Stetter, C.; Kong, L.; Sica, C.; Mailman, R.B.; et al. Susceptibility MRI captures nigral pathology in patients with parkinsonian syndromes. *Mov. Disord.* 2018, 33, 1432–1439.

Retrieved from <https://encyclopedia.pub/entry/history/show/110554>